High-Resolution Solution Structure of Reduced Parsley Plastocyanin†

Stefan Bagby,‖,‡ Paul C. Driscoll,§ Timothy S. Harvey,§,‖ and H. Allen O. Hill*,‡

Received December 22, 1993; Revised Manuscript Received March 21, 1994⊛

ABSTRACT: A high-resolution three-dimensional solution structure of parsley plastocyanin has been determined using ^{1}H-NMR-derived data. An ensemble of 30 conformers has been calculated, exhibiting an atomic root mean square distribution about the mean coordinate positions of 0.37 ± 0.03 Å for backbone atoms and 0.75 ± 0.04 Å for all heavy atoms. (These values exclude residues 8–10 which are disordered.) The global fold of parsley plastocyanin is closely similar to those of other plastocyanins which have been structurally characterized by X-ray diffraction and NMR methods. However, deletion of residues at positions 57 and 58 of the consensus plastocyanin sequence causes elimination of a turn found in most higher plant plastocyanins. This turn is located in an acidic patch binding site, which consists of two clusters of acidic residues at positions 42–45 and 59–61. These residues surround the side chain of Tyr 83, which has been shown to be involved in binding of and electron transfer from cytochrome *f*, one of plastocyanin's physiological partners. The acidic recognition site is further disrupted in parsley plastocyanin by nonconservative substitution of two charged residues at positions 59 and 60. The NMR-derived structures show that E53, E85, and E95 compensate for these substitutions and give parsley plastocyanin an acidic recognition site of similar extent to that of other higher plant plastocyanins. This helps to rationalize observations made during investigations of reaction kinetics [Sykes, A. G. (1985) *Chem. Soc. Rev. 14,* 283–315] and observations made previously in our laboratory during studies of the binding of paramagnetic inorganic transition-metal complexes to the acidic patch recognition site of higher plant plastocyanins [Armstrong, F. A., Driscoll, P. C., Hill, H. A. O., & Redfield, C. (1986) *J. Inorg. Biochem. 28,* 171–180. Driscoll, P. C. (1987) Ph.D. Thesis, University of Oxford].

Plastocyanin (Boulter et al., 1977; Freeman, 1981; Adman, 1985; Sykes, 1985; Sykes, 1991; Gross, 1993) is a small (M_r 10.5 kDa), single polypeptide protein which contains a copper center with characteristic type I properties. Plastocyanin is a mobile shuttle of electrons (Selak & Whitmarsh, 1984) between reduced cytochrome *f* (Gray, 1992) in the cytochrome b_6f complex and pigment $P700^+$ of photosystem I in the photosynthetic electron transport chain of higher plants and algae (Anderson, 1982). Previous structural studies have shown that plastocyanin adopts a β-sandwich fold consisting of eight β-strands, resembling a flattened cylinder (Colman et al., 1978; Guss & Freeman, 1983; Guss et al., 1986; Moore et al., 1988a; Collyer et al., 1990; Moore et al., 1991; Redinbo et al., 1993).

Analysis of the crystal structure of poplar plastocyanin (Colman et al., 1978; Guss & Freeman, 1983; Guss et al., 1986) has indicated that plastocyanin possesses two potential binding sites for physiological redox partners. These have been termed the north site (or hydrophobic patch) and east site (or acidic patch). The former consists of residues that form the rim of the hydrophobic pocket in which the copper site lies. The latter consists of a surface concentration of negatively charged residues located on two kinks in the backbone at sequence positions 42–45 and 59–61.

Of the higher plant plastocyanins, only that from poplar does not have a negatively charged residue at position 45 (Ser instead of Glu). Parsley plastocyanin is unusual in that it does not possess negatively charged residues at positions 59 and 60 (nonconservative substitution of Gln and Pro for Glu and Glu). Alignment of sequences (Figure 1) shows that parsley plastocyanin is further distinguished from most other higher plant plastocyanins by the deletion of residues at positions 57 and 58. (Parsley plastocyanin residues which occur after the deletions at positions 57 and 58 are henceforth

```
                0         5        10        15        20        25        30
Poplar          IDVLLGADDGSLAFVPSEFSISPGEKIVFK
Spinach         VEVLLGGGDGSLAFLPGDFSVASGEEIVFK
Fr. bean        LEVLLGSGDGSLVFVPSEFSVPSGEKIVFK
Parsley         AEVKLGSDDGGLVFSPSSFTVAAGEKITFK
S. obliquus     ANVKLGADSGALVFEPATVTIKAGDSVTWT
E. prolifera    AAIVKLGGDDGSLAFVPNNITVGAGESIEFI
A. variabilis   ETYTVKLGSDKGLLVFEPAKLTIKPGDTVEFL
Conservation          § ‡       ‡  ‡  ‡       ‡   §   §

                     35        40        45        50        55        60
Poplar          NNAGFPHNIVFDEDSIPSGVDASKISMSEE
Spinach         NNAGFPHNVVFDEDEIPSGVDAAKISMSEE
Fr. bean        NNAGFPHNVVFDEDEIPAGVDAVKISMPEE
Parsley         NNAGFPHNIVFDEDEVPAGVNAEKIS**QP
S. obliquus     NNAGFPHNIVFDEDAVPAGVNADALS**HD
E. prolifera    NNAGFPHNIVFDEDAVPAGVDADAIS**AE
A. variabilis   NNKVPPHNVVFDAALNPAKSADLAKSLSHK
Conservation    § §   § ‡ ‡ ‡    ‡ ‡ § §   ‡  § §   § § ‡

                     65        70        75        80        85        90
Poplar          DLLNAKGETFEVALSNKGEYSFYCSPHQGA
Spinach         DLLNAPGETYKVTLTEKGTYKFYCSPHQGA
Fr. bean        ELLNAPGETYVVTLDTKGTYSFYCSPHQGA
Parsley         EYLNGPGETYEVTLTEKGTYKFYCEPHAGA
S. obliquus     DYLNAPGESYTAKFDTAGEYGYFCEPHQGA
E. prolifera    DYLNSKGQTVVRKLTTPGTYGVYCDPHSGA
A. variabilis   QLLMSPGQSTSTTFDAAGEYTFYCEPHRGA
Conservation      ‡ §   ‡ §     §  §     ‡  ‡  § § ‡  ‡ ‡  ‡ ‡

                     95       100
Poplar          GMVGKVTVN
Spinach         GMVGKVTVN
Fr. bean        GMVGKVTVN
Parsley         GMKGEVTVN
S. obliquus     GMVGKVIVQ
E. prolifera    GMKMTITVQ
A. variabilis   GMVGKITVAG
Conservation    ‡ ‡  §  § § ‡
```

FIGURE 1: Plastocyanin amino acid sequences. An asterisk indicates a deletion, ‡ indicates an invariant residue, and § indicates a residue which is invariant in higher plant plastocyanins.

† This is a contribution from the Oxford Centre for Molecular Sciences, of which H.A.O.H. is a member. P.C.D. is a Royal Society University Research Fellow. The U.K. Medical Research Council and Science and Engineering Research Council are thanked for financial support.

‡ Inorganic Chemistry Laboratory.

§ Department of Biochemistry.

‖ Present address: Division of Molecular and Structural Biology, Ontario Cancer Institute, 500 Sherbourne Street, Toronto, Ontario, Canada M4X 1K9.

⊛ Abstract published in *Advance ACS Abstracts,* May 1, 1994.

0006-2960/94/0433-6611$04.50/0

Table 1: Proton Resonance Assignments[a]

res	NH	$C^{\alpha}H$	$C^{\beta}H$	$C^{\gamma}H$	$C^{\delta}H$	other
A1		4.07	1.33			
E2[b]	8.63	5.04	1.85, 1.93	2.10, 2.10		
V3	8.80	4.27	1.38	1.07, –0.15		
K4	9.04	4.72	1.66, 1.90	1.29, 1.29		$C^{\epsilon}H$, 3.67, 3.67
L5	8.68	4.03	0.91, 2.35	1.54	0.81, 0.91	
G6	8.05	4.21, 5.10				
S7	8.80	4.51	3.67, 4.24			
D8[b]	8.82	4.20	2.58, 2.76			
D9[b]	7.94	4.55	2.60, 2.80			
G10	8.04	3.28, 4.15				
G11	7.86	3.60, 3.84				
L12	8.48	4.23	0.94, 1.71	1.57	0.25, 0.63	
V13	7.11	4.78	2.23	0.56, 0.85		
F14	8.91	4.80	2.63, 3.12		7.08	$C^{\epsilon}H$, 7.22; $C^{\zeta}H$, 7.22
S15	8.82	5.04	3.34, 3.80			
P16		5.05	2.28, 2.59	1.53, 1.92	3.53, 3.70	
S17	8.32	4.60	4.43, 4.46			
S18	7.52	5.80	3.80, 3.83			
F19	7.88	5.11	3.14, 3.36		6.83	$C^{\epsilon}H$, 6.93; $C^{\zeta}H$, 6.65
T20	8.50	5.50	3.99	1.13		
V21	8.89	4.71	2.17	0.71, 0.88		
A22	7.92	4.78	1.39			
A23	8.52	3.93	1.27			
G24	8.66	3.17, 4.25				
E25	8.17	4.22	2.10, 2.25	2.21, 2.35		
K26	8.32	4.21	1.55, 1.58	1.09, 1.16	1.48, 1.48	
I27	9.13	4.28	1.77	0.62, 1.85	0.79	$C^{\gamma}H_3$, –0.01
T28	8.31	4.65	3.88	1.12		
F29	9.59	5.26	2.82, 3.31		7.18	$C^{\epsilon}H$, 6.76; $C^{\zeta}H$, 6.00
K30	9.13	4.86	1.44, 1.69	1.20, 1.45	1.55, 1.55	$C^{\epsilon}H$, 2.78, 2.78
N31	9.13	5.12	2.72, 2.78			$N^{\delta}H$, 5.29, 6.80
N32	9.13	5.19	2.35, 3.48			$N^{\delta}H$, 7.66, 7.83
A33	9.05	5.19	1.33			
G34[b]	8.80	3.45, 3.49				
F35	5.66	3.16	3.07, 3.15		6.79	$C^{\epsilon}H$, 7.24; $C^{\zeta}H$, 7.39
P36		5.02	1.53, 2.39	1.71, 1.93	3.52, 3.70	
H37	7.24	5.70	2.61, 3.53		7.70	$C^{\epsilon}H$, 7.06; $N^{\epsilon}H$, 11.50
N38	9.98	4.41	3.70, 3.73		6.84, 7.25	
I39	6.69	4.25	1.25	0.13, 1.08	0.43	$C^{\gamma}H_3$, –0.28
V40	9.02	3.96	1.09	0.58, 0.68		
F41	8.54	4.59	2.72, 2.80		7.23	$C^{\epsilon}H$, 7.00; $C^{\zeta}H$, 6.61
D42	8.49	4.57	2.44, 2.95			
E43	8.51	3.97	2.08, 2.20	2.30, 2.37		
D44	8.60	4.83	2.70, 2.84			
E45	8.16	4.70	1.69, 2.36	1.98, 2.22		
V46	6.93	4.82	1.76	0.80, 1.28		
P47		4.24	1.43, 2.33	1.22, 1.35	2.10, 2.50	
A48	8.15	4.12	1.36			
G49	8.52	3.61, 4.21				
V50	7.66	3.85	2.11	0.78, 0.83		
N51[b]	8.55	4.95	2.70, 2.97			$N^{\delta}H$, 7.20, 7.72
A52	9.12	3.80	1.43			
E53	8.55	4.40	2.78, 2.82	1.76, 1.80		
K54	7.48	4.28	1.90, 2.02	1.47, 1.58	1.72, 1.72	$C^{\epsilon}H$, 2.93, 2.93
I55	6.95	4.47	1.70	0.99, 1.07	–0.12	$C^{\gamma}H_3$, 0.73
S56	7.33	4.68	4.10, 4.65			$O^{\gamma}H$, 5.84
Q59	9.23	4.75	1.06, 1.15	–0.03, 2.50		
P60		4.20	2.18, 2.46	1.90, 1.98	3.20, 3.78	
E61	7.74	4.00	1.77, 1.87	2.18, 2.25		
Y62	7.81	4.36	2.72, 2.91		7.00	$C^{\epsilon}H$, 6.75
L63	9.20	4.46	1.30, 1.68	1.68	0.66, 0.74	
N64	8.37	4.61	2.65, 2.73			$N^{\delta}H$, 6.69, 7.46
G65	8.08	3.49, 3.97				
A66	8.42	3.44	1.42			
G67	8.38	3.64, 4.17				
E68	7.10	4.30	2.03, .11	1.91, 2.28		
T69	8.28	5.74	4.07	1.14		
Y70	8.88	5.04	2.59, 3.28		6.74	$C^{\epsilon}H$, 7.12
E71	7.80	5.50	1.63, 1.77	2.08, 2.13		
V72	8.75	4.37	1.90	0.93, 1.03		
T73	8.02	4.48	3.75	0.81		
L74	8.93	4.57	0.92, 1.56	1.30	–0.28, 0.31	
T75	8.58	4.21	4.12	1.00		
E76	7.78	4.39	1.92, 2.24	1.96, 2.06		
K77	8.59	4.01	1.72, 1.90	1.30, 1.60	1.70, 1.70	$C^{\epsilon}H$, 3.01, 3.01
G78	8.59	3.86, 4.63				
T79	8.38	5.17	3.85	1.12		
Y80	9.60	5.59	2.97, 3.62		7.12	$C^{\epsilon}H$, 6.57; $O^{\eta}H$, 10.32

Table 1: (Continued) Proton Resonance Assignments[a]

res	NH	$C^{\alpha}H$	$C^{\beta}H$	$C^{\gamma}H$	$C^{\delta}H$	other
K81	8.26	5.11	1.90, 2.12	1.38, 1.61	1.70, 1.70	$C^{\epsilon}H$, 2.94, 2.94
F82	7.83	5.38	1.57, 1.76		6.18	$C^{\epsilon}H$, 5.87; $C^{\zeta}H$, 6.89
Y83	9.24	5.21	3.12, 3.20		6.77	$C^{\epsilon}H$, 6.63
C84	7.75	5.21	2.93, 3.24			
E85	9.84	4.39	2.24, 2.43	2.34, 2.59		
P86		4.17	0.99, 1.74	1.09, 1.37	3.29, 5.16	
H87	8.35	5.18	3.40, 3.79		7.00	$C^{\epsilon}H$, 7.59
A88[b]	8.55	4.18	1.59			
G89[b]	9.14	3.89, 3.93				
A90	7.58	4.61	1.62			
G91	8.01	3.79, 4.46				
M92	7.68	4.65	1.81, 2.28	1.65, 2.07		$C^{\epsilon}H_3$, 0.51
K93	8.06	5.16	1.87, 2.14	1.51, 1.84	1.66, 1.66	
G94	8.42	2.90, 4.58				
E95	8.29	5.09	1.78, 1.90	1.75, 2.10		
V96	9.08	4.95	1.22	0.30, 0.82		
T97	8.22	5.00	3.94	1.05		
V98	9.25	4.66	2.43	0.62, 0.66		
N99	8.92	4.70	2.63, 2.70			$N^{\delta}H$, 6.47, 7.23

[a] pH 7.3, 35 °C. [b] NH–$C^{\alpha}H$ cross peak not observed at 35 °C; NH shift from 20 °C spectrum.

referred to by two numbers: for the first, the deletions are included in the residue count, for the second the deletions are omitted from the count.) In these respects, parsley plastocyanin is similar to plastocyanins from green algae: *C. fusca*[1] (Kelly & Ambler, 1974), *E. prolifera* (Simpson et al., 1986), and *S. obliquus* (Kelly & Ambler, unpublished work, reported in Sykes, 1985) plastocyanins retain acidic residues at positions 42–44, but Met 57 and Ser 58 of poplar plastocyanin are deleted, and Glu 59 of poplar plastocyanin is replaced by Ala or His. Additional differences from most other plant plastocyanins which the parsley protein shares with these algal plastocyanins are the occurrence of a tyrosine at position 62 and a glutamate at position 85, compared to Leu 62 and Ser 85 of poplar plastocyanin, for example (Figure 1). The amino acid sequences of plastocyanins from barley (Nielsen & Gausing, 1987), rice (Yano et al., 1989), and carrot (Shoji et al., cited in Yano et al., 1989) have been shown to have features that are more in common with parsley plastocyanin than most other sequenced higher plant plastocyanins. For example, barley plastocyanin has deletions at positions 57 and 58, a tyrosine at position 62, and a glutamate at position 85.

Both NMR and kinetic studies (Sinclair-Day et al., 1986; Jackman et al., 1987) indicate that the pK_{α} of the copper ligand His 87 is significantly higher in parsley plastocyanin than in other higher plant plastocyanins, suggesting a more polar environment for this residue in parsley plastocyanin. For example, values obtained by NMR and kinetic methods of 5.7 and 5.5 for parsley plastocyanin compare with 4.9 and 4.8 for spinach plastocyanin.

Detailed NMR studies of parsley plastocyanin have been undertaken in order to determine the effects of its sequence differences (Figure 1) on overall fold and particularly on the structure of the acidic binding site. Essentially complete sequential resonance assignments have been obtained using standard methodology (Wüthrich, 1986). These assignments have been used to obtain distance and dihedral angle restraints, permitting calculations of a high-resolution three-dimensional structure of parsley plastocyanin. This structure is compared with those previously obtained by X-ray crystallography for the plastocyanins from poplar (Colman et al., 1978; Guss & Freeman, 1983; Guss et al., 1986) and *E. prolifera* (Collyer et al., 1990) and by NMR for French bean plastocyanin (Moore et al., 1991).

EXPERIMENTAL PROCEDURES

Isolation and Purification of Parsley Plastocyanin. Parsley plastocyanin was isolated and purified by a modification of the method developed by Plesnicar and Bendall (1970). FPLC (Pharmacia) was used for further purification. A 120-mg sample of protein with a purity ratio (A_{597}/A_{278}) of 1.5 was obtained from 10 kg of frozen dry parsley. Plastocyanin samples for NMR experiments were approximately 2 mM in protein and were prepared using a previously described procedure (Driscoll et al., 1987).

NMR Experiments and Data Processing. NMR spectra were acquired in a phase-sensitive manner using a Bruker AM600 spectrometer, with time-proportional phase incrementation (Marion & Wüthrich, 1983) for quadrature detection in t_1. NOESY (Jeener et al., 1979; Macura et al., 1981) spectra were recorded in D_2O at temperatures of 35 and 20 °C and in H_2O at 35, 20, and 15 °C. Mixing times of 200, 175, 150, 125, and 60 ms were used. In the case of the experiments with 60-ms mixing time, zero quantum coherence effects were minimized with a 10% (D_2O) or 5% (H_2O) random variation of the mixing time. HOHAHA (Braunschweiler & Ernst, 1983; Davis & Bax, 1985; Bax & Davis, 1985; Bax, 1989) spectra were recorded in D_2O at 35 and 20 °C and in H_2O at 35, 20, and 15 °C. Initial HOHAHA spectra (D_2O sample) were recorded with an MLEV-17$_y$ spin-lock sequence sandwiched between 2.5-ms trim pulses. Subsequent experiments in D_2O and H_2O utilized a WALTZ-17$_y$ anisotropic mixing sequence bracketed by 1.5- and 3-ms trim pulses. Mixing times ranged from 34 to 54 ms. D_2O spectra were recorded at pH 7.3 (uncorrected meter reading) and those in H_2O at pH 7.3 and 6.5.

For most NOESY spectra in H_2O, a semiselective "jump and return" sequence ($90°_x - \tau - 90°_{-x}$) (Plateau & Guéron, 1982) in place of the final 90° pulse, was used to suppress the

[1] Abbreviations: *C. fusca*, *Chlorella fusca*; *E. prolifera*, *Enteromorpha prolifera*; *S. obliquus*, *Scenesdemus obliquus*; *C. reinhardtii*, *Chlamydomonas reinhardtii*; FPLC, fast protein liquid chromatography; NOESY, two-dimensional nuclear Overhauser enhancement spectroscopy; HOHAHA, two-dimensional homonuclear Hartmann–Hahn spectroscopy; MLEV, Malcolm Levitt; WALTZ, wideband alternating-phase low-power technique for zero residue splitting; DQF COSY, double quantum filtered two-dimensional correlation spectroscopy; PECOSY, primitive exclusive two-dimensional correlation spectroscopy; NOE, nuclear Overhauser effect; COSY, two-dimensional correlation spectroscopy; rms, root mean square; rmsd, root mean square deviation.

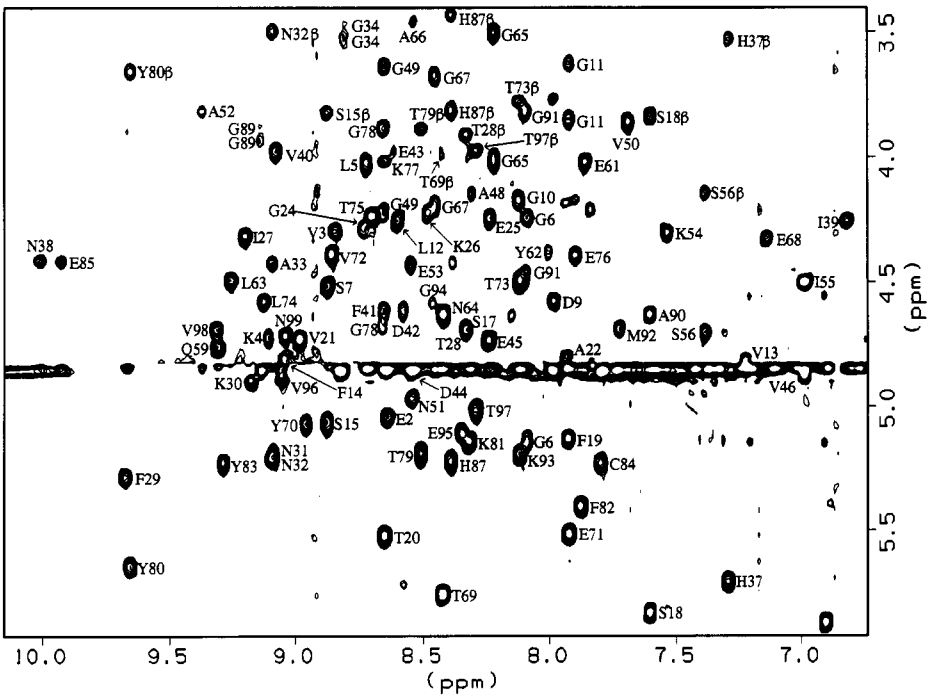

FIGURE 2: Fingerprint region from a HOHAHA spectrum recorded at 20 °C, pH 7.3, with a 34-ms WALTZ-17$_y$ mixing sequence.

water resonance. For most HOHAHA spectra in H_2O, suppression of the water resonance was achieved using the sequence of Bax et al. (1987). Time-domain deconvolution was used to remove the residual water signal (Marion et al., 1989). Other NOESY and HOHAHA spectra in H_2O were recorded with presaturation of the water resonance. Spectra in D_2O were recorded with presaturation of the residual HOD resonance. In all cases, baseline distortions in F_2 were minimized by optimizing the receiver phase and preacquisition delay (Marion & Bax, 1988a). Typically, 700–1024 increments of 2K data points were collected per experiment, with 32 scans per increment. Digital resolution was approximately 4 Hz/point in each dimension after zero filling. For all NOESY and HOHAHA spectra, a line-broadening parameter of −15 to −25 Hz and a Lorentz-to-Gaussian resolution enhancement parameter of 0.15, 0.20, or 0.25 were applied in F_2 and a 60° or 70° phase-shifted sine-squared bell was applied in F_1.

DQF COSY spectra (Rance et al., 1983) were recorded at 35 °C in both D_2O and H_2O, with a phase cycle for removal of artifacts due to rapid pulsing (Derome & Williamson, 1988). Selective irradiation during the relaxation delay period was used to suppress the solvent resonance. A total of 1024 increments of 4K data points were acquired. An unshifted sine bell window function was applied in both dimensions. For the purpose of accurate measurement of $^3J_{\alpha N}$ and $^3J_{\alpha\beta}$ (valyl) coupling constants, zero filling was employed to increase the digital resolution to 0.86 Hz/point in F_2 and 3.44 Hz/point in F_1.

PECOSY (Müller, 1987; Marion & Bax, 1988b) spectra were recorded at 35 °C in D_2O and H_2O and at 42 °C in D_2O. A total of 1024 increments of 4K data points were collected, with a spectral width of 7.35 kHz. An unshifted sine bell window function was applied in both dimensions. Zero filling yielded a digital resolution of 0.90 Hz/point in F_2 and 3.6Hz/point in F_1.

All data processing was carried out using the Hare Research software package FELIX.

Distance Restraints. Interproton distance restraints were obtained from the NOESY experiments detailed above. Experiments were carried out under a variety of conditions in order to reduce the problem of spectral overlap. Lower temperature H_2O experiments also allowed the observation of fingerprint cross peaks for those residues with more rapidly exchanging backbone amide protons.

All NOEs were classified as strong, medium or weak, corresponding to upper limits of 2.7, 3.3, and 5.0 Å in the interproton distance restraints. Upper limits of distances involving methyl groups, nonstereospecifically assigned methylene protons, and C^δ and C^ϵ protons of phenylalanine and tyrosine were corrected for center averaging (Wüthrich et al., 1983). An additional 0.5 Å was added to the upper limits for distances involving methyl groups (Wagner et al., 1987; Clore et al., 1987).

Copper Restraints. Since NMR does not furnish direct evidence of metal coordination, the copper atom was omitted from initial calculations until the structures were of sufficiently high quality to identify the copper-binding residues. These were identified as His 37, Cys 84(82), His 87(85), and Met 92(90). Calculations with restraints that allow copper coordination through either the N^δ or N^ϵ of the His imidazole rings, and which keep the imidazole rings and copper coplanar, indicated that both His residues ligate through the N^δ atoms. As in the case of French bean plastocyanin (Moore et al., 1991), this bonding arrangement is supported by the observation of the $N^\epsilon H$ resonance of His 37 (Table 1). Copper was subsequently incorporated with restraints to ensure that the imidazole rings and copper were coplanar and that the overall coordination geometry was approximately tetrahedral. Also, equilibrium bond distance restraints of 2.12 ± 0.2, 2.15 ± 0.2, 2.40 ± 0.2, and 2.90 ± 0.2 Å were employed for the Cu-N^δ(His 37), Cu-S^γ(Cys 84(82)), Cu-N^δ(His 87(85)), and Cu-S^δ(Met 92(90)) interactions. These restraints were treated in the same way as NOE-derived distance restraints in the structure calculations.

Structure Calculations. Structure calculations were carried out iteratively, employing a successively larger experimental data set. Initial ambiguities among distance restraints could

Table 2: Stereospecific Assignments of β-Methylene Protons[a] and $^3J_{\alpha\beta}$ Coupling Constants

residue	β_1 (ppm)	β_2 (ppm)	$^3J_{\alpha\beta1}$ (Hz)	$^3J_{\alpha\beta2}$ (Hz)
Glu 2	1.85	1.93	2.5	9.2
Leu 5	0.91	2.35	3.7	14.0
Ser 7	3.67	4.24	4.4	4.4
Asp 8			3.0	12.4[b]
Asp 9			5.8	4.9[b]
Leu 12	0.94	1.71	3.5	13.9
Phe 14	2.63	3.12	2.7	11.4
Ser 15	3.34	3.80	5.4	10.7
Phe 19	3.14	3.36	4.3	5.4
Glu 25	2.25	2.10	11.2	5.0
Phe 29	2.82	3.31	2.5	13.0
Lys 30			7.4	9.5[c]
Asn 31			6.9	4.8[c]
Asn 32			6.6	13.6[b]
His 37	3.53	2.61	4.0	12.0
Asp 44	2.84	2.70	4.0	13.0
Glu 45	2.36	1.69	3.8	10.3
Asn 51			7.6	9.8[c]
Glu 61(59)			10.3	6.2
Tyr 62(60)	2.72	2.91	2.6	11.4
Leu 63(61)	1.68	1.30	3.4	12.2
Asn 64(62)			10.7	4.5[b]
Glu 68(66)			9.8	10.9[c]
Tyr 70(68)	3.28	2.59	6.6	11.3
Glu 71(69)	1.63	1.77	5.6	10.6
Leu 74(72)	0.92	1.56	4.5	12.6
Glu 76(74)				11.0
Tyr 80(78)	2.97	3.62	3.0	11.0
Lys 81(79)	2.12	1.90	4.7	12.0
Phe 82(80)	1.57	1.76	5.2	2.5
Tyr 83(81)	3.20	3.14	3.1	12.0
Cys 84(82)	2.93	3.24	6.8	11.2
Glu 85(83)			10.7	6.8[c]
His 87(85)	3.79	3.40	4.3	12.6
Lys 93(91)			7.9	4.9[c]
Glu 95(93)			5.7	7.2[c]

[a] For residues not represented, $^3J_{\alpha\beta}$ values could not be measured in the PECOSY spectrum due to low intensity or absence of cross peaks, due to degeneracy or near degeneracy of C^β protons, or due to overlap with cross peaks from other residues. [b] NOE and $^3J_{\alpha\beta}$ data were insufficient to give an unambiguous answer in STEREOSEARCH. [c] Motional averaging and a mixture of rotamer populations present.

Table 3: Stereospecific Assignments of Valine and Leucine Methyl Groups

residue	$C^{\gamma1}H_3$ or $C^{\delta1}H_3$	$C^{\gamma2}H_3$ or $C^{\delta2}H_3$	$^3J_{\alpha\beta}$ (Hz)	conformation
Val 3	1.07	−0.15	10.9	g^+
Leu 5	0.91	0.81		
Leu 12	0.63	0.25		
Val 13	0.85	0.56	2.9	g^-
Val 21	0.88	0.71	2.1	g^-
Val 40	0.68	0.58	10.6	g^+
Val 46	0.80	1.28	4.0	t
Val 50			10.6	g^+
Leu 63(61)	0.66	0.74		
Val 72(70)	0.93	1.03	3.9	
Leu 74(72)	−0.28	0.31		
Val 96(94)	0.82	0.30	5.5	t
Val 98(96)	0.62	0.66	11.3	g^+

often be resolved by analysis of low-resolution structures. The protocols employed for the calculations used the program X-PLOR (Brünger et al., 1987; Brünger, 1988). Dynamical simulated annealing was used to fold polypeptide chains with random backbone dihedral angles (Nilges et al., 1988, 1991), and the resulting structures were refined using further cycles of dynamical simulated annealing. The methods used were identical to those described in detail previously (Hommel et al., 1992). Structures were displayed on a Silicon Graphics system using InsightII (Biosym Technology, San Diego, CA).

RESULTS

Sequential Resonance Assignments. Essentially complete ^1H resonance assignments (Table 1) were obtained using standard methodology (Wüthrich, 1986). Stereospecific assignments of β-methylene protons and of methyl groups of valine and leucine residues are shown in Tables 2 and 3. The fingerprint region from a HOHAHA spectrum is shown with backbone assignments in Figure 2.

Dihedral Angles and Stereospecific Assignments. φ torsion angle restraints were obtained from $^3J_{HN\alpha}$ coupling constants, which for all non-glycine residues were measured in high digital resolution DQF COSY spectra using spectral simulations (Redfield & Dobson, 1990; Smith et al., 1991), to correct for the discrepancy between measured and actual $^3J_{NH\alpha}$ values arising from finite linewidths. A stretch of three or more residues with $^3J_{HN\alpha} < 5$ Hz was taken to indicate the presence of α secondary structure, and the φ torsion angle was assigned a value of −65 ± 25°. β secondary structure was inferred for $^3J_{HN\alpha} > 9$ Hz, and the φ torsion angle was then assigned a value of −120 ± 40° (Pardi et al., 1984).

χ_1 torsion angle restraints and stereospecific assignment of prochiral β-methylene protons (Table 2) were initially obtained on the basis of $^3J_{\alpha\beta}$ coupling constants and intraresidue NOEs involving the backbone amide, C^α and C^β protons. Values of the $^3J_{\alpha\beta}$ coupling constants of non-valyl residues were determined as passive coupling constants, where possible, from the relative displacement of cross-peak components in PE-COSY (Müller, 1987; Marion & Bax, 1988b) spectra recorded in D_2O. When a preferred rotamer position of a side chain was identified, corresponding to χ_1 = 60°, 180°, or −60° (Wagner et al., 1987), the torsion angle restraint was described by a square well effective potential function (Clore et al., 1986) of width ±20–40° about the rotamer positions (Driscoll et al., 1989). Based on this qualitative analysis, stereospecific assignments were obtained for 23 of the 49 nondegenerate β-methylene proton pairs in parsley plastocyanin (Table 2).

In cases where both $^3J_{\alpha\beta}$ coupling constants had values of 5–9 Hz, indicative of motional averaging, conformational heterogeneity (i.e., a mixture of rotamer populations) about the C^α–C^β bond was assumed and neither stereospecific assignment nor χ_1 torsion angle restraint was obtained. This was the case for six of the pairs of β-methylene protons for which $^3J_{\alpha\beta}$ coupling constants could be determined: Lys 30, Asn 31, Asn 51, Glu 68(66), Lys 93(91), and Glu 95(93) (see introduction for an explanation of the numbering scheme). For residues Lys 4, Asp 42, Glu 43, Lys 54, Gln 59(57), Lys 77(75), Met 92(90), and Asn 99(97), no $^3J_{\alpha\beta}$ coupling constants could be obtained, due to low cross-peak intensity or complete absence of one or both αβ cross peaks. For other residues, the $^3J_{\alpha\beta}$ coupling constants could not be measured due to chemical shift degeneracy or near degeneracy of the C^β protons, or due to overlap with cross peaks from other residues. This was the case for Ser 17, Ser 18, Asn 38, Phe 41, and Glu 53.

Subsequent to qualitative studies, the program STEREO-SEARCH (Kraulis et al., 1989; Nilges et al., 1990) was used to obtain stereospecific assignments of β-methylene protons and φ, ψ, and χ_1 dihedral angle restraints. The data base employed was a systematic one with idealized geometry. The results agreed with the qualitatively determined stereospecific assignments. The minimum ranges employed for φ, ψ, and χ_1 dihedral angle restraints were ±30°, ±50°, and ±20° (Kraulis et al., 1989).

Stereospecific assignments were obtained for the methyl groups of eight of the nine valine residues (Table 3), using $^3J_{\alpha\beta}$ coupling constants [from high digital resolution DQF

Table 4: Comparison of Hydrogen Bonding in Reduced Poplar and Parsley Plastocyanins

poplar donor and acceptor	parsley donor and acceptor	slow exchange	poplar donor and acceptor	parsley donor and acceptor	slow exchange
		A. Backbone–backbone			
I1 N–K26 O	A1 N–K26 O	N	I55 N–A52 O	I55 N–A52 O	N
V3 N–V28 O	V3 N–T28 O[a]	Y	S56 N–A52 O	S56 N–A52 O	N
L4 N–V15 O	K4 N–S15 O[a]	Y	M57 N–I39 O	*c*	*d*
L5 N–K30 O	L5 N–K30 O[a]	Y	E61 N–S58 O	*c*	N
G6 N–V13 O	G6 N–V13 O[a]	Y	L63 N–H37 O	L63 N–H37 O	N
A7 N–S11 O	S7 N–G11 O[a]	Y	G67 N–N31 O	G67 N–N31 O	N
G10 N–S7 O	G10 N–S7[e]	N	E68 N–A65 O	E68 N–A65 O	N
V15 N–L4 O	S15 N–K4 O[a]	Y	F70 N–F29 O	Y70 N–F29 O[a]	Y
F19 N–K95 O	F19 N–E95 O[a]	Y	V72 N–I27 O	V72 N–I27 O[a]	Y
I21 N–T97 O	V21–T97 O[a]	Y	G78 N–V98 O	G78 N–V98 O[a]	Y
c	A23 N–N99 O	N	Y80 N–V96 O	Y80 N–V96 O[a]	Y
G24 N–L74 O	G24 N–L74 O[e]	N	S81 N–S45 O	K81 N–E45 O	Y
E25 N–S22 O	E25 N–A22 O[a]	Y	F82 N–G94 O	F82 N–G94 O[a]	Y
I27 N–V72 O	I27 N–V72 O[a]	Y	Y83 N–V40 O	Y83 N–V40 O[a]	Y
V28–N–L1 O	T28 N–A1 O[a]	Y	C84 N–M92 O	C84 N–M92 O[a]	Y
F29 N–F70 O	F29 N–Y70 O[a]	Y	H87 N–C84 O	H87 N–C84 O	N
K30 N–V3 O	K30 N–V3 O[a]	Y	Q88 N–C84 O	A88 N–C84 O	N
N31 N–E68 O	N31 N–E68 O	N	Q88 N–S85 O	A88 N–E85 O	N
N32 N–L5 O	N32 N–L5 O	N	A90 N–H87 O	A90 N–H87 O	N
A33 N–L5 O	A33 N–L5 O	N	G91 N–Q88 O	G91 N–Q88 O	N
H37 N–L63 O	H37 N–L63 O[a]	Y	M92 N–H87 O	M92 N–H87 O	N
I39 N–M57 O	*c*	Y	G94 N–F82 O	G94 N–F82 O[a]	Y
V40 N–Y83 O	V40 N–Y83 O[a]	Y	K95 N–S17 O	E95 N–S17 O[a]	Y
D42 N–S81 O	D42 N–K81 O[a]	Y	V96 N–Y80 O	V96 N–Y80 O[a]	Y
S45 N–D42 O	S45 N–D42 O[a]	Y	T97 N–F19 O	T97 N–F19 O[a]	Y
V50 N–P47 O	V50 N–P47 O[e]	N	V98 N–G78 O	V98 N–G78 O[a]	Y
K54 N–D51 O	K54 N–D51 O	N	N99 N–I21 O	N99 N–V21 O	N
		B. Backbone–Side Chain and Side Chain–Backbone			
S11 N–D9 $O^{\delta 1}$	G11 N–D9 $O^{\delta 1}$ [e]	N	S53 O^{γ}–D51 O^{δ}	*c*	*d*
S11 O^{γ}–D9 O^{δ}	*c*	*d*	S56 O^{γ}–A52 O	S56 O^{γ}–A52 O[a]	Y
N31 $N^{\delta 2}$–L63 O	*b*	Y	S58 N–D61 O^{δ}	*c*	*d*
N31 $N^{\delta 2}$–A65 O	N31 $N^{\delta 2}$–G65 O	Y	S58 O^{γ}–E60 O^{ϵ}	*c*	*d*
N32 $N^{\delta 2}$–G6 O	N32 $N^{\delta 2}$–G6 O	Y	E60 N–S58 O^{γ}	*c*	*d*
H37 $N^{\epsilon 2}$–A33 O	H37 $N^{\epsilon 2}$–A33 O	Y	N64 N–E68 O^{ϵ}	N64 N–E68 O^{ϵ} [e]	N
N38 N–C84 S^{γ}	N38 N–C84 $S^{\gamma \alpha}$	Y	A65 N–E68 O^{ϵ}	G65 N–E68 O^{ϵ} [e]	N
N38 $N^{\delta 2}$–D61 O	*b*	Y	Y80 O^{η}–N76 O	Y80 O^{η}–E76 O	Y
D44 N–D42 O^{δ}	D44 N–D42 O^{δ}	N	S85 N–N38 $O^{\delta 1}$	E85 N–N38 $O^{\delta 1}$	N
S53 N–D51 O^{δ}	*c*	N	N99 $N^{\delta 2}$–I21 O	N99 $N^{\delta 2}$–V21 O	Y

[a] Hydrogen bond used as restrained in structure calculations. [b] Hydrogen bond not predicted or not found. [c] Hydrogen bond not possible due to difference in sequence. [d] Does not apply: donor is not an exchangeable proton or is not found in the parsely plastocyanin sequence. [e] Presence of hydrogen bond uncertain due to low definition of structure.

COSY spectra by spectral simulation (Redfield & Dobson, 1990; Smith et al., 1991)] and the relative intensities of intraresidue NH–C$^{\gamma}$H and C$^{\alpha}$H–C$^{\gamma}$H NOEs (Zuiderweg et al., 1985). During later structure calculations, when the side chains exhibited well-defined conformations, stereospecific assignments were obtained for the methyl groups of all four leucine residues (Table 3) and for the C$^{\alpha}$ protons of nine of the 12 glycine residues (Kline et al., 1988).

Hydrogen Bonds. Sixty distance restraints corresponding to 30 backbone–backbone NH–CO hydrogen bonds were obtained (Table 4). Fifty-four of these were for interstrand hydrogen bonds and six for hydrogen bonds in turns. Also included were four distance restraints for the hydrogen bonds between the hydroxyl proton of Ser 56 and the backbone carbonyl of Ala 52 and between the cysteinyl sulfur of Cys 84(82) and the backbone NH of Asn 38. Two distance restraints were used for each hydrogen bond, one between the donor heavy atom and the acceptor atom (upper limit of 3.2 Å) and one between the hydrogen and the acceptor atom (upper limit of 2.3 Å).

Quality of the Structures. Thirty final structures were calculated using a total of 1406 approximate interproton distance restraints, 55 ϕ, 41 ψ, 26 χ_1, and 5 proline ω [residues 15–16, 35–36, 46–47, 59(57)–60(58), and 85(83)–86(84)] dihedral angle restraints. Structural statistics and a breakdown of the restraints by type is given in Table 5. Best-fit superpositions of backbone and side chain atoms are shown in Figures 3 and 4, and NOE distribution, residue-based rmsd

Table 5: Structural Statistics and Atomic rms Deviations[a]

	⟨SA⟩	(SA)$_r$
rms deviations from exptl distance restraints (Å)		
all (1406)	0.024 ± 0.002	0.024
sequential ($\|i-j\| = 1$) (340)	0.016 ± 0.001	0.016
medium range ($\|i-j\| \leq 5$) (12)	0.027 ± 0.010	0.027
long range ($\|i-j\| > 5$) (588)	0.027 ● 0.003	0.026
intraresidue (280)	0.022 ● 0.006	0.026
H-bond (64)	0.033 ± 0.004	0.028
Cu (14)	0.045 ± 0.026	0.052
rms deviations from exptl dihedral restraints (deg) (129)	0.380 ● 0.077	0.395
F_{NOE} (kcal mol^{-1})[b]	31.4 ± 4.4	23.1
F_{cdih} (kcal mol^{-1})	0.28 ± 0.13	0.40
F_{repel} (kcal mol^{-1})[c]	25.7 ± 2.00	24.1
E_{L-J} (kcal mol^{-1})	−387 ± 8.7	−413
deviations from idealized covalent geometry		
bonds (Å)	0.007 ± 0	0.007
angles (deg)	2.02 ± 0.004	2.39
impropers (deg)	1.02 ● 0.010	1.02

[a] Notation: ⟨SA⟩ are the thirty final simulated annealing structures, (SA)$_r$ is the restrained minimized mean structure obtained by restrained minimization of the mean structure. The latter was obtained by averaging the coordinates of the 30 individual structures, best fitted to each other (residues 8–10 not included in the fitting procedure). The number of each type of restraint used in the calculations is given in parentheses. [b] F_{NOE} and F_{cdih} were calculated using force constants of 50 kcal mol^{-1} Å^{-2} and 200 kcal mol^{-1} rad^{-2}, respectively. [c] F_{repel} was calculated using a final value of 4.0 kcal mol^{-1} Å^{-4} with the van der Waals hard sphere radii set to 0.8 times those in the parameter set PARALLHSA supplied with X-PLOR (Brünger et al., 1987; Brünger, 1988).

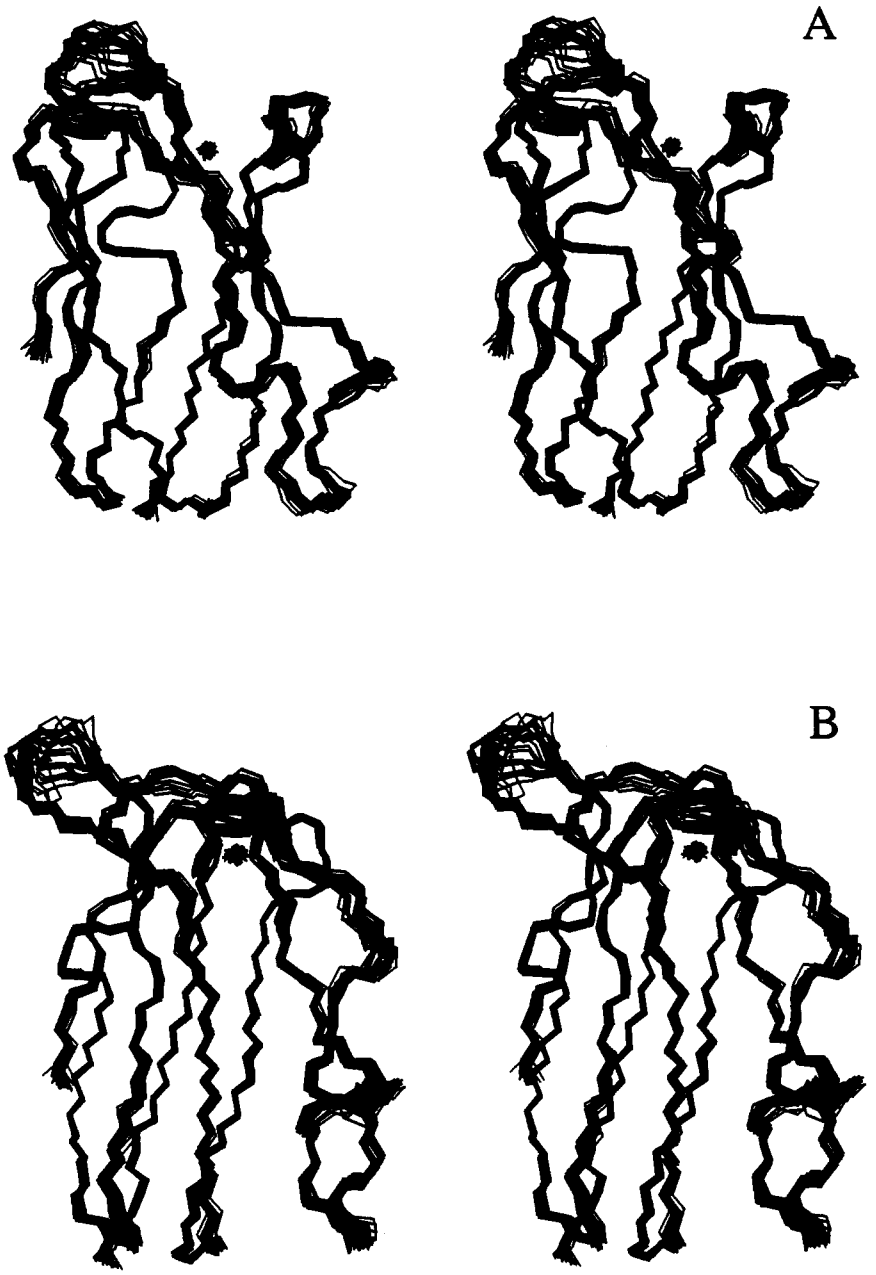

FIGURE 3: (A) Stereoview showing best fit superpositions of the backbone (N, C^{α}, and C′) atoms of the 30 final structures of parsley Cu^{I} plastocyanin. The overlays were generated by fitting atoms of residues mostly in β-strands (residues 1–7, 11–14, 17–21, 25–32, 36–47, 67(65)–74(72), 78(76)–85(83) and 92(90)–99(97)). (B) A view related to that shown in A by an approximately 90° rotation about the *y* axis.

values, and solvent-accessible surface areas are in Figure 5. The data presented in Table 5 and in Figures 3–5 show that good convergence was achieved in the conformational search and that the structures are of high precision. All of the structures showed small deviations from idealized covalent geometry and had favorable nonbonded contacts, as evidenced by a low value of the van der Waals repulsion energy (ranging from 17 to 26 kcal mol^{-1}) and large negative values (−392 ± 7 kcal mol^{-1}) of the Lennard-Jones van der Waals energy (which is not used in the target function for simulated annealing calculations) (Table 5). The structures were subjected to iterative fitting of the backbone atoms (Nilges et al., 1987). Disordered residues 8–10 were ignored in the final fit. The individual structures were refitted to the average structure, termed $\overline{SA}$. $\overline{SA}$ was subjected to 1000 cycles of restrained Powell minimization to optimize geometry and nonbonded contacts, giving the minimized average structure, $(\overline{SA})_r$.

The thirty final structures of reduced parsley plastocyanin exhibit an atomic rms distribution about the mean coordinate positions of 0.37 ± 0.03 Å for backbone atoms and 0.75 ± 0.04 Å for all heavy atoms. These figures exclude residues 8–10, which are disordered. No residual distance restraint violation exceeded 0.29 Å, and only two residual dihedral angle restraint violations were greater than 2.5°. As evidenced by Figures 3 and 5, regions of the parsley plastocyanin backbone exhibiting regular secondary structure are particularly well-defined, whereas loops and turns tend to show a greater variation in conformation, particularly at residues 8–10. Figures 4 and 5 show that side chains in the molecular interior tend to be better defined than those at the surface.

DISCUSSION

Parsley Cu^{I} plastocyanin, in common with other plastocyanins studied by NMR (Driscoll, 1987; Driscoll et al., 1987; Chazin et al., 1988; Chazin & Wright, 1988; Moore et al.,

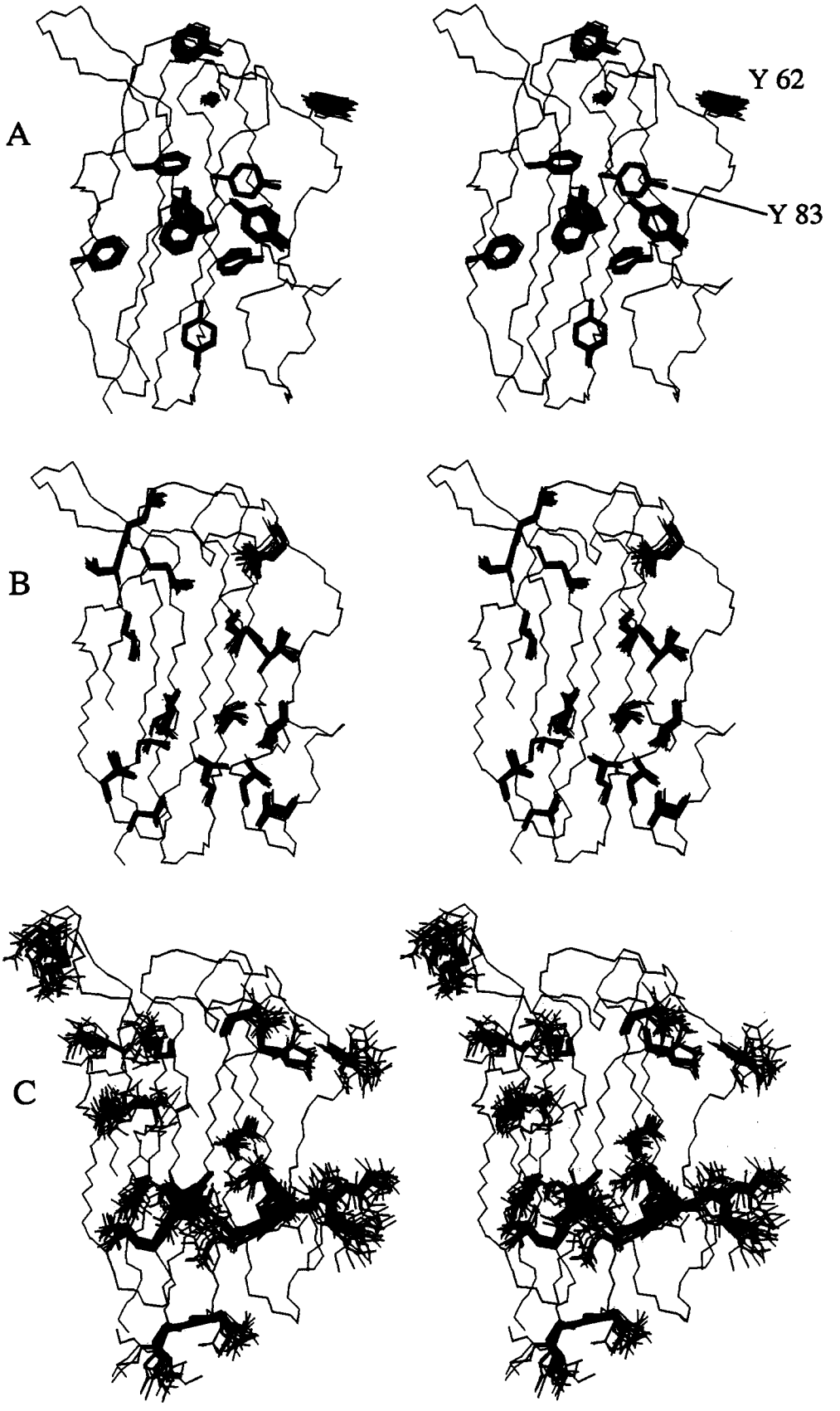

FIGURE 4: Stereoviews of the backbone of one of the calculated structures with (A) aromatic, (B) Val, Leu, and Ile, and (C) Asp, Glu, and Lys side chains of the 30 parsley Cu^{I} plastocyanin structures. N, C^{α}, and C′ atoms of residues 1–7, 11–14, 17–21, 25–32, 36–47, 67(65)–74(72), 78(76)–85(83), and 92(90)–99(97) were superimposed.

1988b), gives spectra with good chemical shift dispersion, sensitivity, and resolution. This facilitates resonance assignment and allows determination of a large number of distance and dihedral angle restraints. The resulting structures are consequently of high quality and precision, especially when it is considered that this study was limited to homonuclear NMR techniques. Many current NMR investigations of similar size polypeptides (about 100 residues) employ ^{15}N-edited NMR experiments, necessitating that the protein be obtained in a recombinant form suitable for ^{15}N-enrichment.

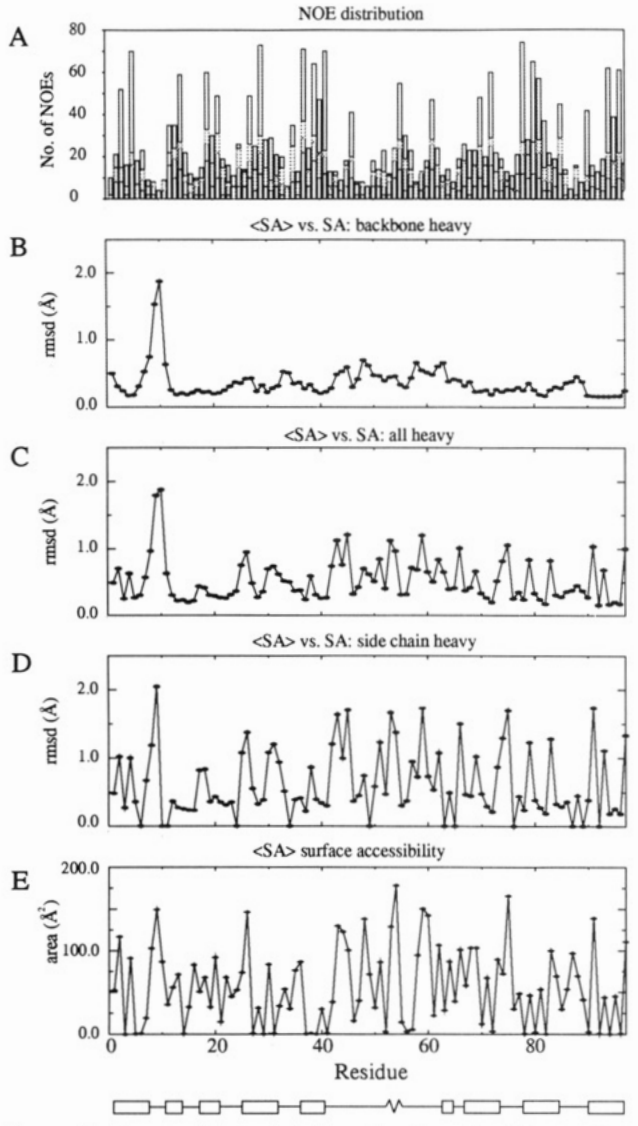

FIGURE 5: Structural data plotted as a function of residue number. (A) NOE distribution, in which each interresidue NOE appears twice, once for each of the two interacting residues. The four categories of NOE, beginning at the bottom of each column, are intraresidue, sequential, medium range ($1 < |i-j| \leq 5$), and long range ($|i-j| > 5$). Average rms d from the mean structure for (B) backbone heavy atoms (N, C^{α}, C′, and O), (C) for all heavy atoms, and (D) for side chain atoms. (E) Solvent-accessible surface area calculated using a 1.6-Å radius probe.

Description of the Structure. The global conformation of reduced parsley plastocyanin (shown in schematic form in Figure 6) is very similar (Figure 7) to those of other structurally characterized plastocyanins (Guss & Freeman, 1983; Guss et al., 1986; Moore et al., 1988a; Collyer et al., 1990; Moore et al., 1991; Redinbo et al., 1993; comparisons with poplar Cu^{I} plastocyanin use the crystal structure obtained at pH 7.0). Thus, the molecule can be described as a β-sandwich, the two faces of which are β-sheets made up by a total of eight β-strands. Pairs of strands are connected by loops or tight turns, and the β-sheets are separated by a hydrophobic core. Sheet I is formed by strands 2A (residues 11–14), 1 (residues 1–7), 3 (residues 25–32), and 6 (residues 67(65)–74(72)). Sheet II consists of strands 2B (residues 17–21), 8 (residues 92(90)–99(97)), 7 (residues 78(76)–85(83)), and 4 (residues 36–41) (Figure 6). The single helical region of the protein, consisting of residues 52–56, is closer to a 3_{10}-helix than a α-helix, consistent with the secondary structure seen in other plastocyanins. The helix is followed by a short strand (residues 62(60)–64(62)). Initial inspection of residues 84(82)–91(89) indicates that these two might be said to form a helix. However, analysis of dihedral angles and putative hydrogen bonds (the relevant residues do not have slowly exchanging amide protons at pH 7.3) indicates that this region is better described as two consecutive β-turns. This is also true of the corresponding regions of poplar and French bean plastocyanins (Guss & Freeman, 1983; Moore et al., 1991). Residues 84-(82)–91(89) of *E. prolifera* plastocyanin form two loops rather than β-turns (Collyer et al., 1990). Additional features which parsley plastocyanin shares with the other structurally characterized plastocyanins include a midstrand type VIb turn (Huber & Steigemann, 1974; Richardson, 1981) at residues 14–17 and a G1 type β-bulge (Richardson et al., 1978) involving residues Gly 6 and Ser 7 of strand 1 and residue Val 13 of strand 2A. There is NOE evidence for the existence of a β-bulge in a similar location in the plastocyanins from French bean (Chazin & Wright, 1988) and *S. obliquus* (Moore et al., 1988b). Poplar plastocyanin does not, however, possess a β-bulge in this location.

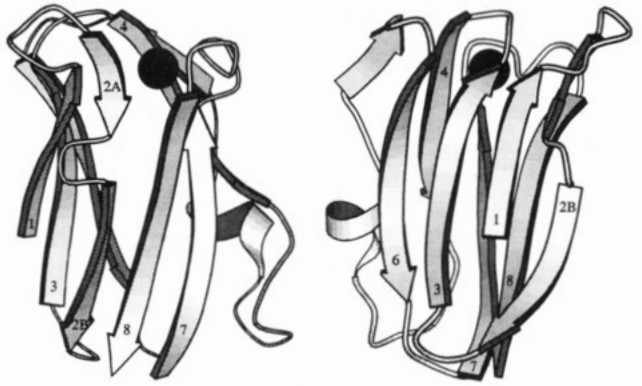

FIGURE 6: Schematic representation of the structure of parsley Cu^{I} plastocyanin. The two views are related by a 100° rotation about the vertical axis. Labels indicate strand numbers. This figure was created using the program MOLSCRIPT (Kraulis, 1991).

The general pattern of β-sheet hydrogen bonding (Table 4) is the same in reduced parsley and poplar plastocyanins, reflecting the close similarity in supersecondary structures (Figure 7). Parsley plastocyanin hydrogen bonds involving amide protons exchanging at intermediate rates were difficult to detect due to the close-to-neutral pH at which H_2O NMR experiments were carried out. This is manifested in the absence of hydrogen-bond restraints in certain parts of the molecule. For example, hydrogen-bond restraints involving the parsley plastocyanin residues corresponding to those in the 84(82)–91(89) β-turns of poplar plastocyanin could not be included in structure calculations (Table 4).

Most of the hydrogen bonds around the copper site of poplar plastocyanin are retained in parsley plastocyanin (Table 4). The retention of one of the hydrogen bonds involving invariant Asn 38, Asn 38N^{δ}H-Glu 61(59)O, seems less certain. The peptide oxygen atom of Glu 61(59) is on the wrong side of a short section of strand (61(59)–64(62)) to form this hydrogen bond. The corresponding peptide oxygen atom has a similar position in *E. prolifera* plastocyanin. This is slightly surprising, given the structural importance attached to this residue in poplar plastocyanin (Guss & Freeman, 1983), and is a consequence of the deletion of residues at positions 57 and 58 in parsley and *E. prolifera* plastocyanins. These deletions also result in elimination of a turn from parsley, *E. prolifera*, and *S. obliquus* plastocyanins (Figure 7). This deletion is of significance since the eliminated turn is located in the acidic patch recognition site (see introduction). This point is discussed further below.

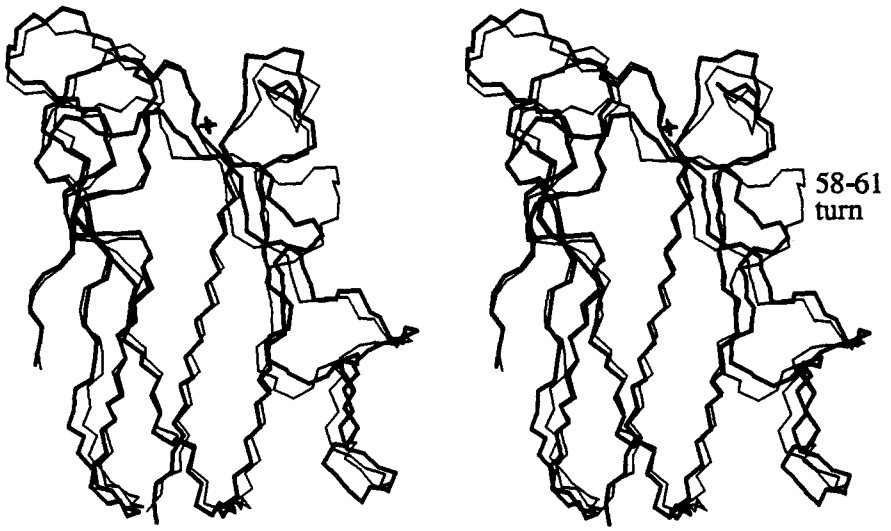

FIGURE 7: Stereoview of a superposition of reduced parsley (narrow line) and poplar plastocyanins. The superposition was generated by fitting backbone heavy atoms (N, C^{α}, and C′) of residues mostly in β-strands (residues 1–7, 11–14, 17–21, 25–32, 36–47, 67(65)–74(72), 78(76)–85(83), and 92(90)–99(97)). Copper is indicated by a cross. The 58–61 turn of poplar plastocyanin is indicated. It can be seen that this turn is eliminated from parsley plastocyanin by deletions at positions 57 and 58.

The hydroxyl proton resonance of Ser 56 is clearly observed in the ^{1}H NMR spectrum of parsley plastocyanin. The calculated structures indicate that there are two potential hydrogen bonds involving this side chain: 56O$^{\gamma}$H-52O and 41NH-56O$^{\gamma}$. Since there is no electrostatic term in the force field used for refinement, it is unlikely that this is an artefact of the modelling method. The 41NH-56O$^{\gamma}$ hydrogen bond was not observed in the crystal structure of poplar plastocyanin (Guss & Freeman, 1983), but is present in the *E. prolifera* plastocyanin crystal structure (Collyer et al., 1990). This difference between the two solid-state structures has been ascribed to sequence differences (Collyer et al., 1990). Resulting changes in side chain volumes allow the helix of *E. prolifera* plastocyanin to move closer to strand 4, permitting the formation of a number of hydrogen bonds. One of these is 41NH-56O$^{\gamma}$, and another involves the side chains of Glu 43 and Asp 53. Such a carboxyl–carboxylate hydrogen bond is thought to result in an anomalously high pK_a (Collyer et al., 1990). This may explain the pK_a of around 5.7 (which is high for protonation at a single carboylate residue) in the reaction of spinach plastocyanin with $Co(phen)_3^{3+}$ as oxidant (Sykes, 1985). The even higher pK_a of parsley (6.1) and *E. prolifera* plastocyanins (ca. 6) may be a reflection of a greater population of conformers possessing an acidic patch carboxyl–carboxylate hydrogen bond relative to most higher plant plastocyanins.

Apart from the presence of a tyrosine at position 62(60), parsley and poplar plastocyanins have aromatic residues in corresponding sequence and spatial positions (Figure 1). The extra aromatic residue at 62(60) of parsley plastocyanin is a characteristic shared with barley and algal plastocyanins such as those from *S. obliquus* and *E. prolifera*. Tyr 62(60) is surface exposed and is located in the northern half of the molecule near the copper site (Figure 4). The solvent-exposed side chain of Tyr 83(81) is involved in 27 distance restraints and is extremely well-defined (Figure 4). It is interesting to note that the crystallographic *B*-factor of the side chain atoms of Tyr 83(81) in the poplar plastocyanin crystal structure is low (ca. 10 Å^2), that the position of this side chain is well-defined in the NMR-derived structures of French bean plastocyanin (Moore et al., 1991), and that the orientation of this side chain is essentially identical in poplar, French bean, *E. prolifera*, and parsley plastocyanins. The precise definition of the aromatic ring of Tyr 83(81) has possible functional significance, given its postulated role in the transmission of electrons to the copper site (see, for example, Roberts et al., 1991), which has been supported by the results of site-directed-mutagenesis studies (He et al., 1991; Modi et al., 1992). These showed that Tyr 83(81) is involved in binding cytochrome *f* and forms part of the electron transfer pathway in reactions with both cytochrome *c* and cytochrome *f*. Theoretical analysis also indicated that the side chain of Tyr 83(81) is part of a potential through-bond electron transfer pathway in *Chlamydomonas reinhardtii* plastocyanin (Redinbo et al., 1993).

The acidic patch, which is a characteristic feature of higher plant plastocyanins, consists of several negatively charged residues located on midstrand β-turns at positions 42–45 and 58–61. The acidic side chains project into solvent, together forming an elongated patch of negative charge which encompasses the solvent-exposed side chain of Tyr 83. The only higher plant plastocyanin for which the Asp-Glu-Asp-Glu sequence at 42–45 is broken is poplar plastocyanin (wherein 45 is serine; Figure 1). Most higher plant plastocyanins have the sequence Glu-Glu-Asp/Glu at positions 59–61. The distinctive acidic patch characteristics described for parsley plastocyanin (see introduction) are common in algal plastocyanins, although the composition of the 58–61 sequence is variable (Figure 1). Any detailed comparison of side chain conformations in this important region may be compromised by the fact that, in parsley and other plastocyanins (Collyer et al., 1990; Redinbo et al., 1993), the acidic side chains are relatively poorly defined (Figure 4). Such disorder is often seen at the molecular surface in NMR-derived structures, and may be associated with relatively high flexibility. This is potentially important for plastocyanin's ability to achieve the correct orientation for electron transfer, since complexes with cytochrome *f* (one of its physiological partners) probably undergo many conformational fluctuations before the required arrangement is achieved (Qin & Kostić, 1993). Despite the relatively low structural definition in this part of the molecule, it is clear that deletion of residues at positions 57 and 58 results in elimination from parsley plastocyanin of the prominent kink seen in poplar and French bean plastocyanins at residues 58–61 (Figure 7). [A similar observation has been made for *E. prolifera* and *C. reinhardtii* plastocyanins (Collyer et al., 1990; Redinbo et al., 1993.)] The two sets of residues constituting the acidic patch are consequently closer to one another than in poplar and French bean plastocyanins. Taking

into account only the 42–45 and 59(57)–61(59) sections, and excluding residue 45 (Ser or Ala, Figure 1) from the poplar and *E. prolifera* plastocyanin calculations, the solvent-accessible surface areas of acidic residues of *E. prolifera*, parsley, poplar, and French bean plastocyanins total 514.5, 542.3, 632.9, and 753.2 Å^2. Such a calculation does not account for the results of previous studies, in which specific paramagnetic broadening effects in the COSY spectra of reduced spinach and parsley plastocyanins were used to delineate the residues bound by paramagnetic inorganic cation complexes and so map out the electrostatic surface of each protein (Armstrong et al., 1986; Driscoll, 1987). No significant difference was detected in the extent of the acidic patch between spinach and parsley plastocyanins (Driscoll, 1987). For both proteins the paramagnetic resonance broadening effects were most noticeable for Tyr 83. Further, the results of extensive kinetic studies by Sykes and co-workers (Chapman et al., 1983; Sinclair-Day & Sykes, 1986; Jackman et al., 1987b; McGinnis et al., 1988) indicate that the reactivity of parsley plastocyanin is not significantly different from that of other higher plant plastocyanins. The paramagnetic resonance broadening effects observed for spinach plastocyanin are probably very similar to those that would be obtained for poplar plastocyanin: there are 22 amino acid differences between the two proteins, mostly involving conservative changes, and NMR studies have shown that the three-dimensional structure of spinach plastocyanin is essentially identical to that of poplar plastocyanin (Driscoll, 1987; Driscoll et al., 1987). In spinach plastocyanin the acidic residues most strongly implicated in cation binding are Asp 42, Glu 43, Asp 44, Glu 45, Asp 51, Glu 59, Glu 60, and Asp 61. The parsley plastocyanin solution structure presented here rationalizes the similarity in the extent of the acidic patch as observed in the paramagnetic probe experiments. Thus the absence of acidic residues at positions 51, 59(57), and 60(58) in parsley plastocyanin appears to be compensated by the presence of acidic residues Glu 53, Glu 85(83), and Glu 95(93). [The corresponding residues in poplar/spinach plastocyanins are Ser/Ala, Ser/Ser, and Lys/Lys (Figure 1.)] When these are included, the total solvent-accessible surface area of acidic residues surrounding Tyr 83(81) of parsley plastocyanin is 816.3 Å^2. [Subtraction of the solvent-accessible surface area of basic Lys 93(91), which corresponds to Val 93 in most other plastocyanins (Figure 1), results in an acidic patch surface area of 677 Å^2. It appears that despite differences in sequence allocation of acidic residues and the deletion of two amino acids, parsley plastocyanin retains an acidic surface of similar extent to other higher plant plastocyanins surrounding residue Tyr 83(81), a residue which seems likely to have a functional role in the electron-transfer pathway (He et al., 1991; Modi et al., 1992).

ACKNOWLEDGMENT

We thank Jonathan Boyd, Nick Soffe, and Christina Redfield for maintenance of NMR spectrometers and assistance with NMR experiments.

REFERENCES

Adman, E. T. (1985) in *Metalloproteins* (P. M. Harrison, Ed.) Part I, pp 1–42, Macmillan.

Anderson, J. M. (1982) *FEBS Lett. 138*, 62–66.

Armstrong, F. A., Driscoll, P. C., Hill, H. A. O., & Redfield, C. (1986) *J. Inorg. Biochem. 28*, 171–180.

Bax, A. (1989) *Methods Enzymol. 176*, 151–168.

Bax, A., & Davis, D. G. (1985) *J. Magn. Reson. 63*, 207–213.

Bax, A., Sklenář, V., Gronenborn, A. M., & Clore, G. M. (1987) *J. Am. Chem. Soc. 109*, 6511–6513.

Boulter, D., Haslett, B. G., Peacock, D., Ramshaw, J. A. M., & Scawen, M. D. (1977) *Int. Rev. Biochem. 13*, 1–40.

Braunschweiler, L., & Ernst, R. R. (1983) *J. Magn. Reson. 53*, 521–528.

Brünger, A. T. (1988) *X-PLOR Manual*, Yale University, New Haven, CT.

Brünger, A. T., Clore, G. M., Gronenborn, A. M., & Karplus, M. (1987) *Protein Eng. 1*, 399–406.

Chapman, S. K., Sanemasa, I., & Sykes, A. G. (1983) *J. Chem. Soc. Dalton Trans.* 2549–2553.

Chazin, W. J., & Wright, P. E. (1988) *J. Mol. Biol. 202*, 623–636.

Chazin, W. J., Rance, M., & Wright, P. E. (1988) *J. Mol. Biol. 202*, 603–622.

Clore, G. M., Nilges, M., Sukumaran, D. K., Brünger, A. T., Karplus, M., & Gronenborn, A. M. (1986) *EMBO J. 5*, 2729–2735.

Clore, G. M., Gronenborn, A. M., Nilges, M., & Ryan, C. (1987) *Biochemistry 26*, 8012–8023.

Clore, G. M., Robien, M. A., & Gronenborn, A. M. (1993) *J. Mol. Biol. 231*, 82–102.

Collyer, C. A., Guss, J. M., Sugimura, Y., Yoshizaki, F., & Freeman, H. C. (1990) *J. Mol. Biol. 211*, 617–632.

Colman, P. M., Freeman, H. C., Guss, J. M., Murata, M., Norris, V. A., Ramshaw, J. A. M., & Venkatappa, M. P. (1978) *Nature 272*, 319–324.

Davis, D. G., & Bax, A. (1985) *J. Am. Chem. Soc. 107*, 2821–2822.

Derome, A. E., & Williamson, M. P. (1990) *J. Magn. Reson. 88*, 177–185.

Dimitrov, M. I., Donchev, A. A., & Egorov, T. A. (1990) *FEBS Lett. 265*, 141–145.

Driscoll, P. C. (1987) D. Phil. Thesis, University of Oxford.

Driscoll, P. C., Hill, H. A. O., & Redfield, C. (1987) *Eur. J. Biochem. 170*, 279–292.

Driscoll, P. C., Gronenborn, A. M., & Clore, G. M. (1989) *FEBS Lett. 243*, 223–233.

Freeman, H. C. (1981) In *Coordination Chemistry-21* (Laurent, J. L., Ed.) pp 29–51, Pergamon Press, New York.

Gray, J. C. (1992) *Photosynth. Res. 34*, 359–374.

Gross, E. L. (1993) *Photosynth. Res. 37*, 103–116.

Guss, J. M., & Freeman, H. C. (1983) *J. Mol. Biol. 169*, 521–563.

Guss, J. M., Harrowell, P. R., Murata, M., Norris, V. A., & Freeman, H. C. (1986) *J. Mol. Biol. 192*, 361–387.

He, S., Modi, S., Bendall, D. S., & Gray, J. C. (1991) *EMBO J. 13*, 4011–4016.

Hommel, U., Harvey, T. S., Driscoll, P. C., & Campbell, I. D. (1992) *J. Mol. Biol. 227*, 271–282.

Huber, R., & Steigemann, W. (1974) *FEBS Lett. 48*, 235–237.

Jackman, M. P., McGinnis, J., Sykes, A. G., Freeman, H. C., Collyer, C. A., & Murata, M. (1987a) *J. Chem. Soc., Dalton Trans.* 2573–2577.

Jackman, M. P., Sinclair-Day, J. D., Sisley, M. J., Sykes, A. G., Denys, L. A., & Wright, P. E. (1987b) *J. Am. Chem. Soc. 109*, 6443–6449.

Jeener, J., Meier, B. H., Bachmann, P., & Ernst, R. R. (1979) *J. Chem. Phys. 71*, 4546–4553.

Kelly, J., & Ambler, R. P. (1974) *Biochem. J. 143*, 681–690.

Kline, A. D., Braun, W., & Wüthrich, K. (1988) *J. Mol. Biol. 204*, 675–724.

Kraulis, P. J. (1991) *J. Appl. Crystallogr. 24*, 946–950.

Kraulis, P. J., Clore, G. M., Nilges, M., Jones, T. A., Pettersson, G., Knowles, J., & Gronenborn, A. M. (1989) *Biochemistry 28*, 7241–7257.

Lappin, A. G. (1981) In *Metal Ions in Biological Systems* (Sigel, H., Ed.) Vol. 13, pp 1–71, Dekker, New York.

Macura, S., Huang, Y., Suter, D., & Ernst, R. R. (1981) *J. Magn. Reson. 43*, 259–281.

McGinnis, J., Sinclair-Day, J. D., Sykes, A. G., Powls, R., Moore, J., & Wright, P. E. (1988) *Inorg. Chem. 27*, 2306–2312.

Marion, D., & Bax, A. (1988a) *J. Magn. Reson. 79*, 352–356.
Marion, D., & Bax, A. (1988b) *J. Magn. Reson. 80*, 528–533.
Marion, D., & Wüthrich, K. (1983) *Biochem. Biophys. Res. Commun. 113*, 967–974.
Marion, D., Ikura, M., & Bax, A. (1989) *J. Magn. Reson. 84*, 425–430.
Modi, S., He, S., Gray, J. C., & Bendall, D. S. (1992) *Biochim. Biophys. Acta 1101*, 64–68.
Moore, J. M., Case, D. A., Chazin, W. J., Gippert, G. P., Havel, T. F., Powls, R., & Wright, P. E. (1988a) *Science 240*, 314–317.
Moore, J. M., Chazin, W. J., Powls, R., & Wright, P. E. (1988b) *Biochemistry 27*, 7806–7816.
Moore, J. M., Lepre, C. A., Gippert, G. P., Chazin, W. J., Case, D. A., & Wright, P. E. (1991) *J. Mol. Biol. 221*, 533–555.
Müller, L. (1987) *J. Magn. Reson. 72*, 191–196.
Nielsen, P. S., & Gausing, K. (1987) *FEBS Lett. 225*, 159–162.
Nilges, M., Clore, G. M., & Gronenborn, A. M. (1987) *FEBS Lett. 219*, 11–16.
Nilges, M., Clore, G. M., & Gronenborn, A. M. (1988) *Protein Eng. 2*, 27–38.
Nilges, M., Clore, G. M., & Gronenborn, A. M. (1990) *Biopolymers 29*, 813–822.
Nilges, M., Kuszewski, J., & Brünger, A. T. (1991) In *Computational Aspects of the Study of Biological Macromolecules by Nuclear Magnetic Resonance Spectroscopy* (Hoch, J. C., Poulsen, F. M., & Redfield, C., Eds.), pp 451–455, Plenum Press, New York.
Pardi, A., Billeter, M., & Wüthrich, K. (1984) *J. Mol. Biol. 180*, 741–751.
Plateau, P., & Guéron, M. (1982) *J. Am. Chem. Soc. 104*, 7310–7311.
Plesnicar, M., & Bendall, D. S. (1970) *Biochim. Biophys. Acta 216*, 192–199.
Qin, L., & Kostić, N. M. (1993) *Biochemistry 32*, 6073–6080.
Rance, M., Sørensen, O. W., Bodenhausen, G., Wagner, G., Ernst, R. R., & Wüthrich, K. (1983) *Biochem. Biophys. Res. Commun. 117*, 458–479.
Redfield, C., & Dobson, C. M. (1990) *Biochemistry 29*, 7201–7214.
Redinbo, M. R., Cascio, D., Choukair, M. K., Rice, D., Merchant, S., & Yeates, T. O. (1993) *Biochemistry 32*, 10560–10567.
Richardson, J. S. (1981) *Adv. Protein Chem. 34*, 167–339.
Richardson, J. S., Getzoff, E. D., Richardson, D. C. (1978) *Proc. Natl. Acad. Sci. U.S.A. 75*, 2574–2578.
Roberts, V. A., Freeman, H. C., Olson, A. J., Tainer, J., & Getzoff, E. D. (1991) *J. Biol. Chem. 266*, 13431–13441.
Selak, M. A., & Whitmarsh, J. (1984) *Photochem. Photobiol. 39*, 485–490.
Simpson, R. J., Moritz, R. L., Nice, E. C., Grego, B., Yoshizaki, F., Sugimura, Y., Freeman, H. C., & Murata, M. (1986) *Eur. J. Biochem. 157*, 497–506.
Sinclair-Day, J. D., & Sykes, A. G. (1986) *J. Chem. Soc., Dalton Trans.* 2069–2073.
Smith, L. J., Sutcliffe, M. J., Redfield, C., & Dobson, C. M. (1991) *Biochemistry 30*, 986–996.
Sykes, A. G. (1985) *Chem. Soc. Rev. 14*, 283–315.
Sykes, A. G. (1991) *Struct. Bonding 75*, 175–224.
Wagner, G., Braun, W., Havel, T. F., Schaumann, T., Gō, N., & Wüthrich, K. (1987) *J. Mol. Biol. 196*, 611–639.
Wüthrich, K. (1986) *NMR of Proteins and Nucleic Acids*, Wiley, New York.
Wüthrich, K., Billeter, M., & Braun, W. (1983) *J. Mol. Biol. 169*, 949–961.
Yano, H., Kamo, M., Tsugita, A., Aso, K., & Nosu, Y. (1989) *Protein Seq. Data Anal., 2*, 385–389, and references cited therein.
Zuiderweg, E. R. P., Boelens, R., & Kaptein, R. (1985) *Biopolymers 24*, 601–611.